

Analysis of Transconductance (g_m) in Schottky-Barrier MOSFETs

Sung-Jin Choi, Chel-Jong Choi, Jee-Yeon Kim, Moongyu Jang, and Yang-Kyu Choi

Abstract—This paper experimentally investigates the unique behavior of transconductance (g_m) in the Schottky-barrier metal–oxide–semiconductor field-effect transistors (SB-MOSFETs) with various silicide materials. When the Schottky-barrier height (SBH) or a scaling parameter is not properly optimized, a peculiar shape of g_m is observed. Thus, g_m can be used as a novel metric that exhibits the transition of the carrier injection mechanisms from a thermionic emission (TE) to thermally assisted tunneling (TU) in the SB-MOSFETs. When the local maximum point of g_m is observed, it can be expected that an incomplete transition occurs between TE and TU in SB-MOSFETs. When a dopant-segregation (DS) technique is implemented in the SB-MOSFETs, however, the carrier injection efficiency from the source to the channel is significantly improved, although the SBH is not minimized. As a consequence, the peculiar shape of the g_m disappears, i.e., a complete transition from TE to TU can be enabled by the DS technique.

Index Terms—Current flow mechanism, dopant-segregated SB (DSSB), dopant segregation (DS), erbium silicide, ErSi_{1.7}, platinum silicide, PtSi, Schottky barrier (SB), Schottky-barrier (SB) MOSFET, silicon-on-insulator (SOI), thermionic emission (TE), transconductance, tunneling.

I. INTRODUCTION

SCHOTTKY-BARRIER metal–oxide–semiconductor field-effect transistors (SB-MOSFETs) with silicided source/drain (S/D) junctions have attracted significant interest as an alternative to conventional MOSFETs [1]–[5]. Due to the existence of an additional SB that depends on the energy lineup between the metal Fermi level and the conduction/valence band

Manuscript received July 18, 2010; revised October 31, 2010; accepted November 4, 2010. Date of current version January 21, 2011. This work was supported in part by the IT R&D Program of the Ministry of Knowledge Economy/Korea Evaluation Institute of Industrial Technology (MKE/KEIT) through Project 10035320, Development of Novel 3-D Stacked Devices and Core Materials for the Next-Generation Flash Memory and Project 10029953, Terabit Nonvolatile Memory Development, by the Nano R&D Program through the National Research Foundation of Korea funded by the Ministry of Education, Science and Technology under Grant 2009-0082583, by the National Research Foundation (NRF) under Grant K20901000002-09E0100-00210 funded by the Korea government, and by Samsung Electronics Co., Ltd. The review of this paper was arranged by Editor G. Jeong.

S.-J. Choi, J.-Y. Kim and Y.-K. Choi are with the School of Electrical Engineering and Computer Science, Division of Electrical Engineering, Korea Advanced Institute of Science and Technology (KAIST), Daejeon 305-701, Republic of Korea (e-mail: ykchoi@ee.kaist.ac.kr).

C.-J. Choi is with the School of Semiconductor and Chemical Engineering, Semiconductor Physics Research Center (SPRC), Chonbuk National University, Jeonju 561-756, Korea.

M. Jang is with the Advanced I-MEMS Team, Electronics and Telecommunications Research Institute (ETRI), Daejeon 305-350, Korea.

Color versions of one or more of the figures in this paper are available online at <http://ieeexplore.ieee.org>.

Digital Object Identifier 10.1109/TED.2010.2092778

of the semiconductor, the mechanism of carrier injection of the SB-MOSFETs—thermionic emission (TE) and thermally assisted tunneling (TU)—considerably differs from that of a conventional MOSFET with doped S/D junctions by ion implantation. However, the SB problematically obstructs the attainment of the best intrinsic performance achievable in conventional MOSFETs [6], [7]. Although PtSi provides a reasonably low Schottky-barrier height (SBH) for *p*-type devices, an ideal candidate for *n*-type devices is still lacking, although rare-earth (RE)-based silicides are known to show the lowest SBH. However, the SBH still remains exceedingly high [8], [9]. Previous work by Knoch *et al.* developed the simplified differential equation as follows [6, Fig. 2]:

$$\frac{d^2\Phi(x)}{dx^2} - \frac{\Phi(x) - V_G + V_{bi}}{\lambda^2} = \frac{\rho_{tot}(x)}{\epsilon_{Si}} \quad \lambda = \sqrt{\frac{\epsilon_{Si}}{\epsilon_{OX}} t_{Si} t_{OX}}$$

where $\Phi(x)$ is the potential variation in the SB-MOSFETs, and V_{bi} is the built-in voltage between the Schottky S/D and the silicon channel, and λ is the screening length or the scaling parameter. Therefore, in the subthreshold regime ($\rho \approx 0$), the potential variation at the Schottky S/D is exponentially screened on a scale of λ , which leads to a strong reduction of the Schottky barrier width if the channel thickness t_{Si} and gate oxide thickness t_{OX} values are small. Therefore, a reduction of λ leads to a steep subthreshold slope (SS) that creates sufficient current drivability and a “complete” transition from TE to TU that occurs at the voltage of the source-body flatband V_{sbf} . On the contrary, we can infer that a large value of λ can result in an “incomplete” transition between two injection mechanisms and show the SS that exceeds 60 mV/dec, even in a case that involves a long channel. This behavior can be represented by the well-known parameter, transconductance g_m . When the local maximum point of g_m can be observed, it can be expected that an incomplete transition occurs between TE and TU in SB-MOSFETs. Thus, careful analysis of g_m can show whether the transition is wholly (i.e., a complete transition) or partly (i.e., an incomplete transition) made in the SB-FETs. Consequently, g_m can be used as a new metric for investigating the carrier injection mechanism.

Recently, a dopant-segregation (DS) technique during silicidation to promote carrier injection has been demonstrated, showing that a SB-MOSFET with DS behaves as a bulk-switching conventional MOSFET with full utilization of the advantages of the SB-MOSFET [10], [11]. As a result, the DS technique greatly relaxes the requirements for low-SB materials and hence allows for high-performance SB-MOSFETs [12].

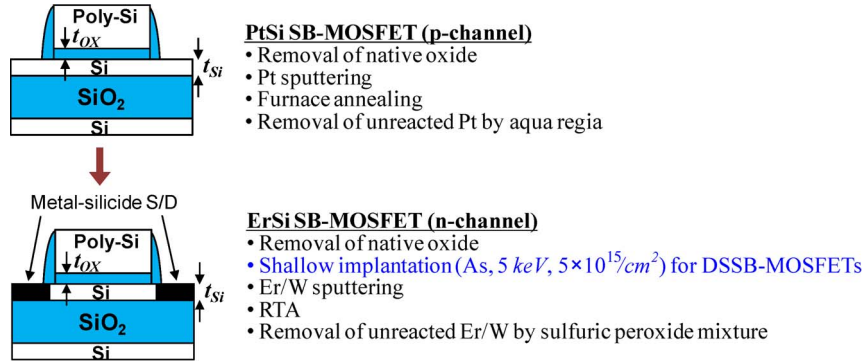


Fig. 1. Process flow of the SB-type devices analyzed in this paper.

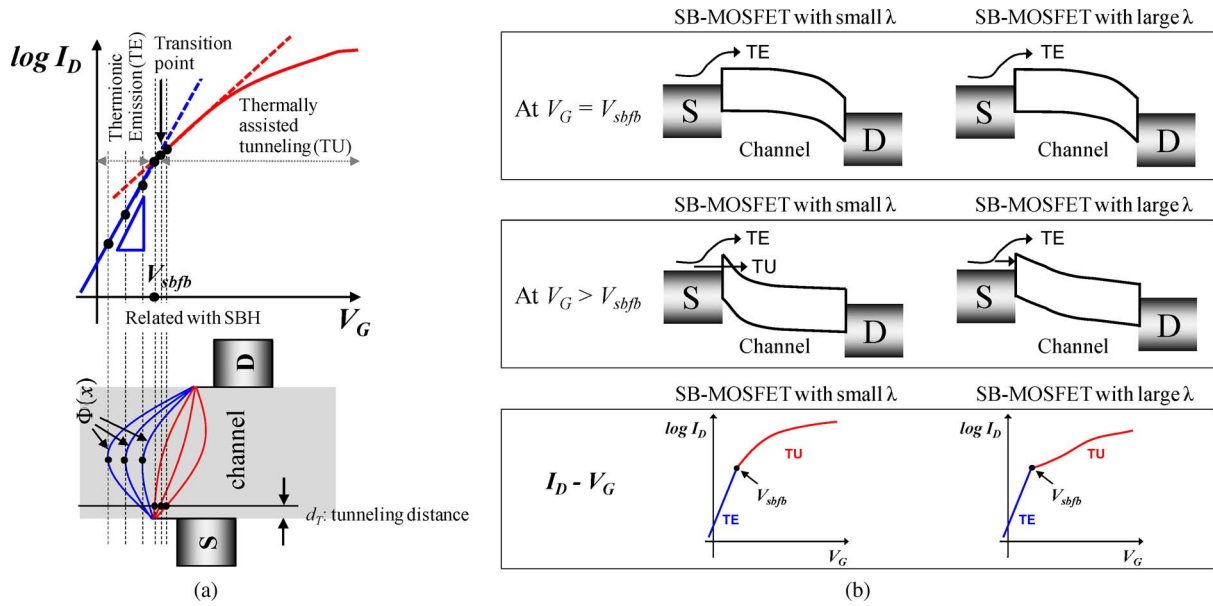


Fig. 2. (a) Conceptual energy diagram and transfer characteristic of the SB-MOSFETs to explain the dominant carrier injection mechanisms. (b) Definition of incomplete and complete transitions through energy diagrams and transfer characteristics. According to the value of λ , the transition between TE to TU can be determined.

This paper investigates the unique characteristic of g_m in both the SB-MOSFET and the dopant-segregated SB-MOSFET (DSSB-MOSFET). Although there have been several reports that describe the various characteristics and physics of the SB- and DSSB-MOSFETs, a comprehensive analysis of the peculiar behavior of g_m in the SB-MOSFET is rare. Here, λ is intentionally enlarged to analyze the carrier injection mechanism. By analyzing the g_m in the SB- and DSSB-MOSFETs with a large λ and discussing the relevant physics behind the observed behaviors in detail, the carrier injection mechanism in SB- and DSSB-MOSFETs are comparatively studied.

II. RESULTS AND DISCUSSION

A SB-MOSFET was initially fabricated on a silicon-on-insulator (SOI) substrate that consisted of a p-channel PtSi S/D and an n-channel ErSi_{1.7} S/D with a gate oxide thickness (t_{ox}) of 10 nm, a silicon channel thickness (t_{Si}) of 50 nm, and a gate length (L_G) of 2.2 μ m. The process flows of the devices are shown in Fig. 1.

Fig. 2 conceptually shows representative transfer characteristics and energy band diagrams in the SB-MOSFET, particularly the n-channel device. As previously analyzed in [6], the transfer characteristic of the SB-MOSFETs is significantly different from the conventional MOSFETs, i.e., pn-junctions S/D devices, due to the different carrier injection mechanism, such as TE and TU. The curve in Fig. 2(a) exhibits two slopes below the threshold. The part displayed in blue is the TE current alone, which primarily comprised carriers injected from the source over the potential barrier. The red part consists of TE and TU currents. As long as the maximum potential barrier is higher than the SBH in the source, the device behaves like a conventional MOSFET with an SS close to 60 mV/dec. When the conduction band is pushed below the SBH in the source, the current consists of both the TE and the TU component. With an incremental change in V_G , the TE component only slightly changes due to image force lowering. The main increase in current arises from the TU through the SB at the source; therefore, an SS exhibits two different slopes. Therefore, the TU component is strongly dependent on the shape of the SB. As a

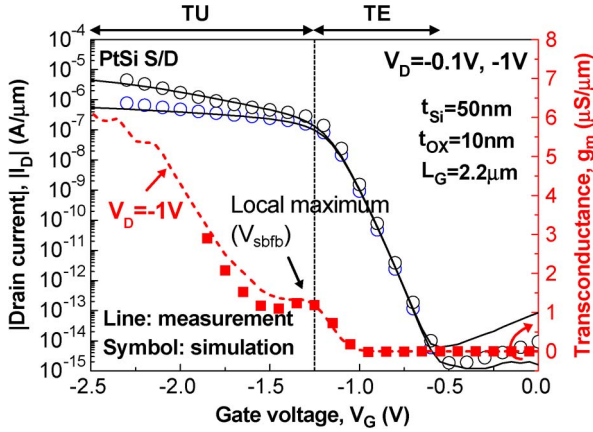


Fig. 3. Transfer characteristics and the g_m of the p -channel PtSi SB-MOSFET. $L_G = 2.2 \mu\text{m}$, $t_{\text{OX}} = 10 \text{ nm}$, and $t_{\text{Si}} = 50 \text{ nm}$. Numerically simulated results are also superimposed. The local maximum of g_m indicates the transition point of the dominant mechanism of the carrier injection between TE and TU.

result, even in the long-channel case, the subthreshold regime of a SB-MOSFET depends on t_S and t_{OX} , i.e., λ . We keep an eye on the fact that the transition of the dominant carrier injection mechanism can occur around the V_{sbfb} . Fig. 2(b) shows the meaning of a complete transition and an incomplete transition by using the energy band diagrams. If a device has a small λ , the transition between the two mechanisms smoothly occurs, resulting in a complete transition between the two mechanisms (i.e., TE and TU). On the other hand, if the device has a large λ , it can be expected that the noticeable transition of carrier injection, i.e., an incomplete transition, occurs around V_{sbfb} . As a result, it can affect the behavior of g_m in the SB-MOSFET, showing a peculiar behavior of the g_m unlike in the conventional MOSFET.

First, the experimental transfer characteristics (I_D - V_G) and the behavior of the g_m in the PtSi SB-MOSFET of the p -channel device are shown in Fig. 3. As shown in this figure, the plot exhibits two slopes in the transfer characteristics, because the dominant mechanism of the carrier injection in each region is different. In the small $|V_G|$ region, the injection of holes is mediated by TE, leading to the steep slope. The injection of holes in the large $|V_G|$ region is dominantly controlled by both TU, leading to a less steepened slope. Interestingly, as expected, the g_m of the PtSi SB-MOSFET significantly differs from that of a conventional MOSFET, in which g_m reaches a peak and then decreases as $|V_G|$ increases due to surface roughness scattering [13]. In the PtSi SB-MOSFET, once V_{sbfb} is reached, g_m reaches a unique “local” maximum, because the effective SBH no longer effectively changes as a function of V_G . Then, as $|V_G|$ further increases over V_{sbfb} , the g_m of the SB-MOSFET again increases and reaches the global maximum. Subsequently, any increase in g_m can be related either to a lowering of the potential energy due to image force effects or to tunneling. Hence, the peculiar behavior of g_m can be attributed to the incomplete transition of the carrier injection mechanism due to the relatively large λ (in this case, λ is approximately 34 nm, considering a single-gate SOI device). This peculiar behavior of g_m can also be found in [14]. If the SB-MOSFET has a small λ value, i.e., thin t_{OX} and t_{Si} in the SOI device,

a complete transition between TE and TU can be possible. As a result, it can be expected that the unique behavior of g_m is no longer observed in the SB-MOSFET with a small λ . This local maximum of g_m is not likely due to leakage from the gate, because the gate current is smaller than 1 pA. To verify that the characteristic behavior of g_m is not caused by unexpected noise during the measurement, the operation of the PtSi SB-MOSFET was numerically simulated based on the same geometry [15]. The calibration of this numerical simulation was referred to in [16]. The simulated results support the measured data and explain the peculiar behavior of g_m . In addition, note that the peculiar behavior of g_m is closely related to the SBH. If the S/D silicide material with large SBH is used at the S/D region of the SB-MOSFET, the peculiar behavior of g_m is hard to be observed, because the transition from TE to TU occurred in a low I_D level.

The specific mechanisms of carrier injection in a SB-MOSFET can easily be analyzed by constructing an Arrhenius plot as a function of V_G to extract the effective SBH for thermal emission alone [17]. The extracted effective SBH of the PtSi SB-MOSFET is shown in Fig. 4. This methodology can be used for the extraction of SBH in SB-MOSFETs by evaluating the variation of effective SBH. It is approximately in the range of 0.23–0.25 eV, which is similar to the extracted SBH of the PtSi from the previously fabricated PtSi SB diode [18]. Clearly, the slope $(\partial\Phi_{\text{SB}}^{\text{eff}}/\partial V_G)^{-1}$ of the effective SBH in the TE region is close to 1 V/V, which indicates that the maximum potential barrier that governs the current flow is not at the interface of the SB but at the middle of the channel. In this region, the SS is analytically determined by $60 \text{ mV/dec} \cdot (\partial\Phi_{\text{SB}}^{\text{eff}}/\partial V_G)^{-1} \approx 60 \text{ mV/dec}$ at room temperature, where $\Phi_{\text{SB}}^{\text{eff}}$ is the effective SBH. Therefore, the PtSi SB-MOSFET behaves as a conventional MOSFET with a steep SS (corresponding to the TE region in Fig. 3). Once the bands are moved below the intrinsic SBH of the PtSi, the injection of the carriers is accomplished mainly by the TU. In this region, the slope of the effective SBH is substantially smaller than unity. Note that the slope at the TU region strongly depends on the λ of the SB-MOSFET. Because the SB now determines the carrier injection, we would expect the SS to be larger than 60 mV/dec (corresponding to the TU region in Fig. 3). The approximate transition point of the injection mechanism between TE and TU is at -1.25 V . In addition, the transition point represents V_{sbfb} and corresponds to V_G when the local maximum of g_m occurs, as also shown in Fig. 3. As $|V_G|$ further increases over V_{sbfb} , only a slight decrease of the effective SBH can occur in the transition region in Fig. 4. As a result, the bump shape (i.e., local maximum) in the g_m characteristic can eventually be observed, as shown in Fig. 3. Hence, the effective SBH as a function of V_G verifies that the unique behavior of the g_m in SB-MOSFETs is due to the incomplete transition between the dominant injection mechanisms in large λ devices. This peculiarity associated with g_m can be a useful metric for analyzing the injection mechanism in SB-type devices.

The total current of SB-MOSFETs comprised a subcomponent by TE and TU as aforementioned. Hence, it can be expected that both components exhibit positive temperature

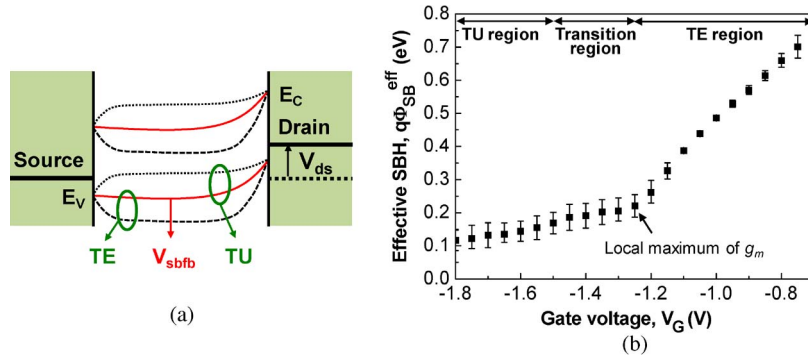


Fig. 4. (a) Energy band diagram for each value of V_{gs} . V_{gs} at the local maximum of g_m corresponds to V_{sbf} . (b) Extracted effective SBH of the PtSi SB-MOSFET when $V_{ds} = -1$ V.

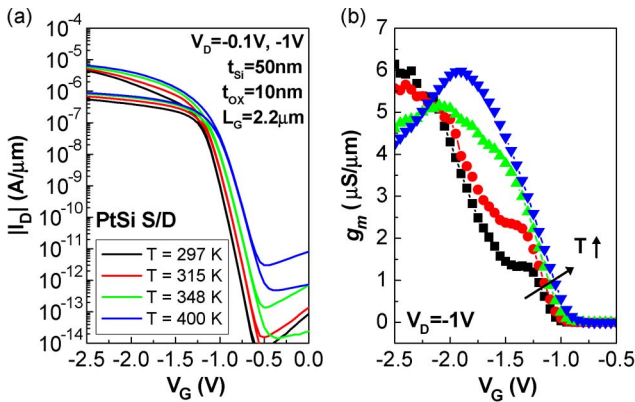


Fig. 5. (a) Transfer characteristics and (b) g_m of the PtSi SB-MOSFET at various temperatures.

dependence and that the TE component has stronger temperature dependence than the TU [19]. As another verification of the origin of the peculiar g_m in SB-MOSFETs, the transfer characteristics were measured for various temperatures, as shown in Fig. 5. As predicted, positive temperature dependence is achieved in the PtSi SB-MOSFET. Moreover, note that the peculiar behavior of g_m changes with the increment of the temperature. As the operating temperature increases, the thermally broadened Fermi distribution function at the source electrode can cause the current to exponentially flow, i.e., the component of TE is increased. Therefore, the g_m value at the local maximum also increases with the temperature. When the temperature exceeds 348 K, however, the barrier height for hole injection at the source interface becomes low enough due to the increased exponential tail of the Fermi level. As a result, the peculiar behavior of g_m disappears. Hence, a similar trend of g_m is observed at high temperature as that of the conventional MOSFET. Based on the analysis of the temperature effect, it is obviously confirmed that the SB between the silicide material and a silicon channel is the primary origin of the behavior of g_m .

The unique behavior of g_m was also observed in the n -channel $\text{ErSi}_{1.7}$ SB-MOSFET, as shown in Fig. 6. $\text{ErSi}_{1.7}$ SB-MOSFETs were fabricated with and without DS to compare the g_m between the two devices, as shown in Fig. 1. The $\text{ErSi}_{1.7}$ SB-MOSFET with DS was implemented in this paper by incorporating the arsenic segregation based on the implantation-before-silicidation (IBS) approach. The association of n -type

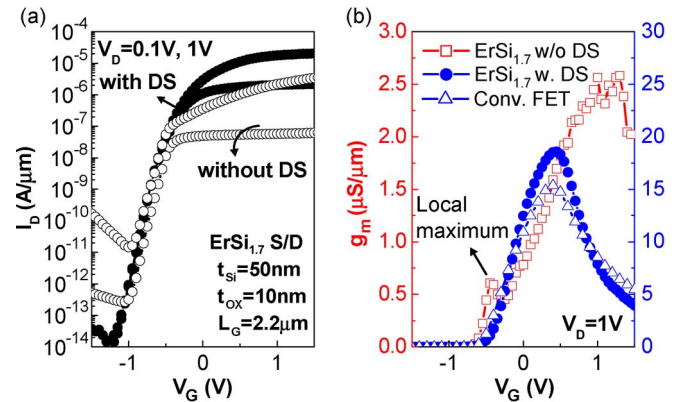


Fig. 6. (a) Transfer characteristics of the n -channel $\text{ErSi}_{1.7}$ SB-MOSFET with and without DS. The device structure of the $\text{ErSi}_{1.7}$ SB-MOSFET with and without DS is identical to a PtSi SB-MOSFET. (b) Value of the g_m of the $\text{ErSi}_{1.7}$ SB-MOSFET with and without DS and a conventional pn-junction MOSFET. The peculiar behavior of the g_m in the $\text{ErSi}_{1.7}$ SB-MOSFET without DS disappears when the DS technique is used.

dopants to a conduction band-edge silicide, e.g., $\text{ErSi}_{1.7}$ and $\text{YbSi}_{1.8}$, has significant importance, because it can take advantage of the low SBH and of the additional barrier lowering and thinning induced by DS. Although this methodology that combines a band-edge silicide to its appropriate dopant type has been demonstrated for p - and n -channel SB-MOSFETs through the implementation of PtSi [20] and $\text{YbSi}_{1.8}$ [21] coupled with boron and arsenic segregation, respectively, the $\text{ErSi}_{1.7}$ with DS has not been demonstrated, as far as we know. Therefore, in this paper, we fabricated $\text{ErSi}_{1.7}$ SB-MOSFETs with and without DS for the evaluation of g_m , even with a large λ , as shown in Fig. 6(a). The perceptible plateau of the g_m at the transition between the TE and TU disappears in the case of the $\text{ErSi}_{1.7}$ SB-MOSFET with DS, as shown in Fig. 6(b), although the devices used here still have a large λ . This condition reveals that the injection is no longer limited by the interface of the SB. In addition, the trend of the g_m in the $\text{ErSi}_{1.7}$ SB-MOSFET with DS is similar to the conventional MOSFET with the same geometrical parameters as SB-MOSFETs with and without DS (e.g., a t_{ox} of 10 nm, a t_{Si} of 50 nm, and a L_G of 2.2 μm). This condition can be understood by considering that the effective SBH is significantly lowered by the heavy doping that arises from DS in the silicide-channel interface, even with a relatively large value of λ . Thus, the analysis of g_m is directly applicable for an understanding of the carrier injection mechanism in

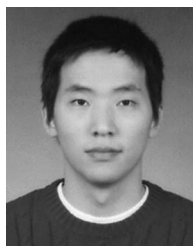
SB-MOSFETs and shows that the use of DS can be a viable means of efficiently improving the electrical performances of SB-MOSFETs.

III. CONCLUSION

The unique behavior of g_m in the SB-MOSFET has been investigated by using an intentionally enlarged λ . In addition, the mechanisms of carrier injection governed by TE and/or TU in a SB-MOSFET with and without DS have been studied and compared through an analysis of the peculiar behavior of g_m , which can be a new metric for analyzing the carrier injection mechanism in SB-MOSFETs. This comparison provided insight into understanding the dominant mechanism of carrier injection, which is affected by λ , temperature, and the DS effect. Being different from the SB-MOSFET, it was experimentally confirmed based on the g_m analysis that the SB-MOSFET with DS behaves as a bulk-switching transistor in a conventional MOSFET due to a drastic reduction of the effective SBH.

REFERENCES

- [1] C. Wang, J. P. Snyder, and J. R. Tucker, "Sub-40-nm PtSi Schottky source-drain metal-oxide-semiconductor field-effect transistors," *Appl. Phys. Lett.*, vol. 74, no. 8, pp. 1174–1176, Feb. 1999.
- [2] J. Kedzierski, P. Xuan, E. H. Anderson, J. Bokor, T.-J. King, and C. Hu, "Complementary silicide source-drain thin-body MOSFETs for 20-nm gate length regime," in *IEDM Tech. Dig.*, 2000, pp. 57–60.
- [3] L. E. Calvet, H. Luebben, M. A. Reed, C. Wang, J. P. Snyder, and J. R. Tucker, "Subthreshold and scaling of PtSi Schottky-barrier MOSFETs," *Superlatt. Microstruct.*, vol. 28, no. 5/6, pp. 501–506, Nov. 2000.
- [4] G. Larrieu and E. Dubois, "Schottky-barrier source/drain MOSFETs on ultrathin SOI body with a tungsten metallic midgap gate," *IEEE Electron Device Lett.*, vol. 25, no. 12, pp. 801–803, Dec. 2004.
- [5] S. Zhu, H. Y. Yu, S. J. Whang, J. H. Chen, C. Shen, C. Zhu, S. J. Lee, M. F. Li, D. S. H. Chan, W. J. Yoo, A. Du, C. H. Tung, J. Singh, A. Chin, and D. L. Kwong, "Schottky-barrier S/D MOSFETs with high-k gate dielectrics and metal-gate electrode," *IEEE Electron Device Lett.*, vol. 25, no. 5, pp. 268–270, May 2004.
- [6] J. Knoch and J. Appenzeller, "Impact of the channel thickness on the performance of Schottky barrier metal-on-semiconductor field-effect transistors," *Appl. Phys. Lett.*, vol. 81, no. 16, pp. 3082–3084, Oct. 2002.
- [7] J. Knoch, M. Zhang, S. Mantl, and J. Appenzeller, "On the performance of single-gated, ultrathin body SOI Schottky-barrier MOSFETs," *IEEE Trans. Electron Devices*, vol. 53, no. 7, pp. 1669–1674, Jul. 2006.
- [8] M. Jang, Y. Kim, J. Shin, S. Lee, and K. Park, "A 50-nm gate-length erbium-silicided n -type Schottky barrier metal-oxide-semiconductor field-effect transistor," *Appl. Phys. Lett.*, vol. 84, no. 5, pp. 741–743, Feb. 2004.
- [9] S. Zhu, J. Chen, M.-F. Li, S. J. Lee, J. Singh, C. X. Zhu, A. Du, C. H. Tung, A. Chin, and D. L. Kwong, " N -type Schottky-barrier source/drain MOSFET using ytterbium silicide," *IEEE Electron Device Lett.*, vol. 25, no. 8, pp. 565–567, Aug. 2004.
- [10] J. Knoch, M. Zhang, Q. T. Zhao, S. Lenk, J. Appenzeller, and S. Mantl, "Effective Schottky-barrier lowering in silicon-on-insulator Schottky-barrier metal-oxide-semiconductor field-effect transistors using dopant segregation," *Appl. Phys. Lett.*, vol. 87, no. 26, pp. 263 505-1–263 505-3, Dec. 2005.
- [11] Q. T. Zhao, U. Breuer, E. Rije, S. Lenk, and S. Mantl, "Tuning of NiSi/Si Schottky-barrier heights by sulfur segregation during Ni silicidation," *Appl. Phys. Lett.*, vol. 86, no. 6, pp. 062 108-1–062 108-3, Feb. 2005.
- [12] J. Kinoshita, Y. Tsuchiya, A. Yagishita, K. Uchida, and J. Koga, "Solution for high-performance Schottky source/drain MOSFETs: Schottky-barrier height engineering with dopant-segregation technique," in *VLSI Symp. Tech. Dig.*, 2004, pp. 168–169.
- [13] H. S. Wong, M. H. White, T. J. Krutsick, and R. V. Booth, "Modeling of transconductance degradation and extraction of threshold voltage in thin-oxide MOSFETs," *Solid State Electron.*, vol. 30, no. 9, pp. 953–968, Sep. 1987.
- [14] R. Valentin, E. Dubois, G. Larrieu, J.-P. Raskin, G. Dambrine, N. Breil, and F. Danneville, "Optimization of RF performance of metallic source/drain SOI MOSFETs using dopant segregation at the Schottky interface," *IEEE Electron Device Lett.*, vol. 30, no. 11, pp. 1197–1199, Nov. 2009.
- [15] *Taurus-Medici User's Manual*, Synopsys, Inc., Mountain View, CA, 2007.
- [16] G. Zhu, X. Zhou, T. S. Lee, L. K. Ang, G. H. See, S. Lin, Y.-K. Chin, and K. L. Pey, "A compact model for undoped silicon-nanowire MOSFETs with Schottky-barrier source/drain," *IEEE Trans. Electron Devices*, vol. 56, no. 5, pp. 1100–1109, May 2009.
- [17] J. Appenzeller, M. Radosavljevic, J. Knoch, and P. Avouris, "Tunneling versus thermionic emission in one-dimensional semiconductors," *Phys. Rev. Lett.*, vol. 92, no. 4, pp. 048 301-1–048 301-4, Jan. 2004.
- [18] M. Jang, Y. Kim, M. Jeon, C. Choi, I. Baek, S. Lee, and B. Park, " N_2 -annealing effects on characteristics of Schottky-barrier MOSFETs," *IEEE Trans. Electron Devices*, vol. 53, no. 8, pp. 1821–1825, Aug. 2006.
- [19] S. Sze, *Physics of Semiconductor Devices*, 2nd ed. New York: Wiley, 1981.
- [20] Z. Zhang, Z. Qiu, P.-E. Hellström, G. B. Malm, J. Olsson, J. Lu, M. Östling, and S.-L. Zhang, "SB-MOSFETs in UTB-SOI featuring PtSi source/drain with dopant segregation," *IEEE Electron Device Lett.*, vol. 29, no. 1, pp. 125–127, Jan. 2008.
- [21] G. Larrieu, D. A. Yarekha, E. Dubois, N. Breil, and O. Faynot, "Arsenic-segregated rare-earth silicide junctions: Reduction of Schottky barrier and integration in metallic n -MOSFETs on SOI," *IEEE Electron Device Lett.*, vol. 30, no. 12, pp. 1266–1268, Dec. 2009.



nanowire electronics.

Sung-Jin Choi received the B.S. degree in electronics and electrical engineering from Chung-Ang University, Seoul, Korea, in 2007 and the M.S. degree from the Korea Advanced Institute of Science and Technology (KAIST), Daejeon, Korea, in 2008. He is currently working toward the Ph.D. degree in electrical engineering in the School of Electrical Engineering and Computer Science, Division of Electrical Engineering, KAIST.

His research interests include Schottky-barrier devices, capacitor-less DRAM, biosensors, and



Chel-Jong Choi received the B.S. degree in ceramic engineering from Hanyang University, Seoul, Korea, in 1997 and the M.S. and Ph.D. degrees in materials science engineering from the Gwangju Institute of Science and Technology (GIST), Gwangju, Korea, in 1999 and 2003, respectively.

From 2003 to 2005, he was with the Samsung Advanced Institute of Technology (SAIT), Suwon, Korea, where he was involved in semiconductor devices and materials characterization. From 2005 to 2008, he was with the Electronics and Telecommunications Research Institute (ETRI), Daejeon, Korea, where he worked on the process development of Schottky-barrier MOSFETs. He is currently an Assistant Professor with the School of Semiconductor and Chemical Engineering, Semiconductor Physics Research Center (SPRC), Chonbuk National University, Jeonju, Korea, where he has been a Faculty Member since 2008. His research interests include nanoscale electronic devices, biosensors, and solar cells.



Jee-Yeon Kim received the B.S. degree from the Korea Advanced Institute of Science and Technology (KAIST), Daejeon, Korea, in 2009. She is currently working toward the M.S. degree in electrical engineering in the School of Electrical Engineering and Computer Science, Division of Electrical Engineering, KAIST.

Her research interests include biosensors and nanowire electronics.



Moongyu Jang received the B.S. degree in physics from Kyungpook National University, Daegu, Korea, in 1991 and the M.S. and Ph.D. degrees in physics from the Korea Advanced Institute of Science and Technology (KAIST), Daejeon, Korea, in 1993 and 1997, respectively.

In 1997, he joined Hyundai Electronics, Inc. (now Hynix Semiconductor, Inc.), Icheon-Si, Korea, where he was involved in the process integration of system-on-chip (SoC) devices. From 1997 to 1998, he was involved in the development of 0.35- μm SoC technology. From 1999 to 2001, he was involved in the development of 0.18- μm SoC technology. In 2001, he joined the Electronics and Telecommunications Research Institute (ETRI), Daejeon, Korea, where he is involved in the basic research on nanoscale devices and is currently with the Advanced I-MEMS Team. His research interests include the processing and analysis of nanoscale MOSFETs, Schottky-barrier MOSFETs, mesoscopic quantum transport phenomena, and silicon-based thermoelectric devices.



Yang-Kyu Choi received the B.S. and M.S. degree from Seoul National University, Seoul, Korea, in 1989 and 1991, respectively, and the Ph.D. degree from the University of California, Berkeley, in 2001.

From January 1991 to July 1997, he was with Hynix Co., Ltd., Kyungki-Do, Korea, where he developed 4-, 16-, 64-, and 256-M DRAM as a Process Integration Engineer. He is currently an Associate Professor with the School of Electrical Engineering and Computer Science, Division of Electrical Engineering, Korea Advanced Institute of Science and Technology (KAIST). He is the author or a coauthor of more than 100 papers and is the holder of seven U.S. patents and 99 Korean patents. His research interests include multiple-gate MOSFETs, exploratory devices, novel and unified memory devices, nanofabrication technologies for bioelectronics, and nanobiosensors. He has also worked on reliability physics and quantum phenomena for nanoscale CMOS.

Dr. Choi received the Sakrison Award for the Best Dissertation from the Department of Electrical Engineering and Computer Sciences, University of California, Berkeley, in 2002 and the Scientist of the Month for July 2006 Award from the Ministry of Science and Technology, Korea. His biographic profile was published in 57th Marquis Who's Who in America.